Check for updates

RESEARCH ARTICLE

TDP-43 Cryptic RNAs in Perry Syndrome: Differences across Brain Regions and TDP-43 Proteinopathies

Sarah R. Pickles, PhD,[1,2] Jesus Gonzalez Bejarano, MSc,[1] Anand Narayan, BSc,[1] Lillian Daughrity, BSc,[1] Candela Maroto Cidfuentes, BSc,[1] Madison M. Reeves, MSc,[1] Mei Yue, BSc,[1] Paula Castellanos Otero, MSc,[1] Virginia Estades Ayuso, MSc,[1,2] Judy Dunmore, BSc,[1] Yuping Song, BSc,[1] Jimei Tong, BSc,[1] Michael DeTure, PhD,[1] Bailey Rawlinson, BSc,[1] Monica Castanedes-Casey, BSc,[1] Jaroslaw Dulski, PhD, MD,[3,4,5] Catalina Cerquera-Cleves, MD, MSc,[6,7] Yongjie Zhang, PhD,[1,2] Keith A. Josephs, MD,[8] Dennis W. Dickson, MD,[1,2] Leonard Petrucelli, PhD,[1,2] Zbigniew K. Wszolek, MD,[3*] and Mercedes Prudencio, PhD[1,2*]

ABSTRACT: Background: Perry syndrome (PS) is a rare and fatal hereditary autosomal dominant neurodegenerative disorder caused by mutations in dynactin (*DCTN1*). PS brains accumulate inclusions positive for ubiquitin, transactive-response DNA-binding protein of 43 kDa (TDP-43), and to a lesser extent dynactin.

Objectives: Little is known regarding the contributions of TDP-43, an RNA binding protein that represses cryptic exon inclusion, in PS. Therefore, we sought to identify the degree of TDP-43 dysfunction in two regions of PS brains.

Methods: We evaluated the levels of insoluble pTDP-43 and TDP-43-regulated cryptic RNAs and protein in the caudate nucleus and substantia nigra of 7 PS cases, 12 cases of frontotemporal lobar degeneration (FTLD) with TDP-43 pathology, and 11 cognitively healthy controls without TDP-43 pathology.

Results: Insoluble pTDP-43 protein levels were detected in PS brains to a similar extent in the caudate nucleus and substantia nigra but lower than those in FTLD brains. The caudate nucleus of PS showed accumulation of eight TDP-43-regulated cryptic RNAs (*ACTL6B*, *CAMK2B*, *STMN2*, *UNC13A*, *KCNQ2*, *ATG4B*, *GPSM2*, and *HDGFL2*) and cryptic protein (HDGFL2) characteristic of FTLD. Conversely, only one cryptic target, *UNC13A*, reached significance in the substantia nigra despite similar pTDP-43 levels.

Conclusion: We detected TDP-43 cryptic RNAs and protein in PS caudate nucleus. Given the importance of cryptic exon biology in the development of biomarkers, and the identification of novel targets for therapeutic intervention, it is imperative we understand the consequences of TDP-43 dysfunction across different brain regions and determine the targets that are specific and common to TDP-43 proteinopathies. © 2025 The Author(s). *Movement Disorders* published by Wiley Periodicals LLC on behalf of International Parkinson and Movement Disorder Society.

Key Words: transactive-response DNA-binding protein of 43 kDa (TDP-43); Perry syndrome; frontotemporal dementia; cryptic; frontotemporal lobar degeneration

[1]Department of Neuroscience, Mayo Clinic, Jacksonville, Florida, USA; [2]Neurobiology of Disease Graduate Program, Mayo Graduate School, Mayo Clinic College of Medicine, Jacksonville, Florida, USA; [3]Department of Neurology, Mayo Clinic, Jacksonville, Florida, USA; [4]Division of Neurological and Psychiatric Nursing, Faculty of Health Sciences, Medical University of Gdansk, Gdansk, Poland; [5]Neurology Department, St Adalbert Hospital, Copernicus PL Ltd., Gdansk, Poland; [6]Department of Neurosciences, Neurology Unit, Hospital Universitario San Ignacio, Bogota, Colombia; [7]CHU de Québec Research Center, Axe Neurosciences, Université Laval, Quebec City, Quebec, Canada; [8]Department of Neurology, Mayo Clinic, Rochester, Minnesota, USA

This is an open access article under the terms of the Creative Commons Attribution-NonCommercial-NoDerivs License, which permits use and distribution in any medium, provided the original work is properly cited, the use is non-commercial and no modifications or adaptations are made.

***Correspondence to:** Dr. Zbigniew K. Wszolek, Department of Neurology, Mayo Clinic, 4500 San Pablo Road S, Jacksonville, FL 32224, USA; E-mail: wszolek.zbigniew@mayo.edu; Dr. Mercedes Prudencio, Department of Neuroscience, Mayo Clinic, 4500 San Pablo Road S, Jacksonville, FL 32224, USA; E-mail: prudencio.mercedes@mayo.edu

Sarah R. Pickles and Jesus Gonzalez Bejarano have contributed equally to this work.

Relevant conflicts of interest/financial disclosures: The authors declare no conflicts of interest relevant to this study.

Funding agencies: This work was supported by the National Institutes of Health (RF1NS120992: K.A.J. and M.P., U54NS123743: L.P. and M.P., R35NS097273: L.P., and R01AG037491: K.A.J.), the Target ALS Foundation (M.P., Y.Z., and L.P.), the BrightFocus Foundation (M.P.), and the Robert Packard Center for ALS Research at Johns Hopkins (L.P.). Z.K.W. is partially supported by the NIH/NIA and NIH/NINDS (1U19AG063911, FAIN: U19AG063911), the Haworth Family Professorship in Neurodegenerative Diseases fund, the Albertson Parkinson's Research Foundation, the PPND Family Foundation, and Margaret N. and John Wilchek Family. J.D. is partially supported by the Haworth Family Professorship in Neurodegenerative Diseases fund (90052067) and receives a "Scholarship for Outstanding Young Scientists" from the Polish Minister of Science (SMN/19/1279/2023). C.C.C. is the recipient of a Vanier Canada Graduate Scholarship from the Canadian Institutes of Health Research.

Received: 10 October 2024; **Revised:** 6 December 2024; **Accepted:** 17 December 2024

Published online 9 January 2025 in Wiley Online Library (wileyonlinelibrary.com). DOI: 10.1002/mds.30104

Perry syndrome (PS) is a rare and fatal hereditary autosomal dominant neurodegenerative disorder. PS patients are characterized by the early development (range of onset of symptoms: 35–61 years) of progressive symptoms of parkinsonism, central hypoventilation, depression, and severe weight loss.[1-6] PS patients usually die of respiratory deficiency, leading to sudden unexplained death or suicide within 5.5 years from disease onset.[3,5,7] Since the original description of PS in a Canadian family in 1975,[8] about 30 new kindreds comprising 160 affected family members have been described.[7] Mutations in the dynactin 1 gene (*DCTN1*) are causative for PS[9] but have also been reported in other neurodegenerative disorders, such as amyotrophic lateral sclerosis (ALS), frontotemporal lobar dementia (FTD), hereditary motor neuropathy type 7b (dHMN7B), and supranuclear palsy.[5,10] *DCTN1* encodes $p150^{glued}$, the largest subunit of the dynactin complex and a component essential for axonal transport.[4] All PS-associated *DCTN1* mutations are located within or adjacent to a highly conserved glycine-rich domain, which mediates microtubule binding.[4] PS-associated mutations in *DCTN1* lead to dopaminergic and serotonergic dysfunction,[11] as well as dynactin redistribution and/or aggregation in vitro.[9] PS brains present neuronal loss and gliosis in several areas of the brain, with the substantia nigra being the most severely affected region and the caudate nucleus and other areas impacted to lesser degrees.[1] Additional neuropathological assessments reveal a lack of Lewy bodies and neurofibrillary tangles,[1] but inclusions positive for ubiquitin, transactive-response DNA-binding protein of 43 kDa (TDP-43) pathology, and dynactin (to a lesser extent) are present in the affected regions.[1,4,7,12] TDP-43 deposits in PS are in the form of neuronal cytoplasmic inclusions (NCI), neuronal intranuclear inclusions, dystrophic neurites, axonal spheroids, oligodendroglial cytoplasmic inclusions, and perivascular astrocytic inclusions.[1,12,13] TDP-43 inclusions in the frontal and temporal cortices and subcortical regions, including the substantia nigra, are also present in cases of frontotemporal lobar degeneration (FTLD).[14-16] TDP-43 is a ubiquitously expressed nuclear protein, with a wide range of functions involving multiple aspects of RNA metabolism,[17] including suppressing the inclusion of "cryptic" intronic sequences into mature RNA, forming "cryptic exons."[18-21] Several of these cryptic RNAs accumulate in the brains of ALS, FTLD, and Alzheimer's disease (AD) cases, in regions with abundant TDP-43 pathology.[22-30] TDP-43-dependent cryptic splicing has yet to be explored in PS. Therefore, we sought to investigate whether TDP-43 cryptic RNA and protein targets observed in FTLD/ALS and AD brains were also present in affected brain regions of PS.

Patients and Methods

Study Participants

Our study included the substantia nigra and caudate nucleus tissue from 7 PS cases, 12 FTLD cases with TDP-43 pathology, and 11 cognitively healthy controls without TDP-43 pathology, which was confirmed by a trained neuropathologist (Table 1). Diagnosis was independently performed by neurologists and neuropathologists upon neurological and pathological examinations, respectively. Tissue was obtained from the Mayo Clinic Florida Brain Bank. All participants, or the next of kin, provided written informed consent, and all protocols were reviewed and approved by the Mayo Clinic Institutional Review Board and Ethics Committee. FTLD cases and controls were matched as best as possible for age at death and sex.

Immunohistochemistry

Paraffin-embedded 5-μm-thick sections from the caudate nucleus and substantia nigra were processed for immunohistochemistry. After deparaffinization in xylene and reagent alcohol, antigen was retrieved by steaming slides in distilled water for 30 minutes. Immunohistochemistry was performed using Dako EnVision reagents (Dako, Carpinteria, CA) and a Dako autostainer. To assess TDP-43 pathology, the caudate nucleus and substantia nigra were examined after immunohistochemistry with an antibody against pTDP-43 (Cosmo Bio Co., Ltd, cat. no. TIP-PTD-M01, 1:5000),

TABLE 1 *Study cohort characteristics*

Variable	Controls (N = 11)	PS (N = 7)	FTLD (N = 12)
Age at death (years)	64.81 (55.3, 77.0)	62.89 (44.3, 69.1)	74.33 (57.5, 84.0)
Sex (females)	6 (54.5%)	3 (42.9%)	6 (50.0%)
Age at onset (years)	NA	55.89 (38.3, 62.08)	62.41 (51.0, 79.8)
Disease duration (years)	NA	6 (3, 7)	7.5 (3, 25)

The sample median (minimum, maximum) is given for continuous variables (age, disease duration), and categorical variables (sex) were summarized with number and percentage of patients.
Abbreviations: PS, Perry syndrome; FTLD, frontotemporal lobar degeneration; NA, not applicable.

15318257, 2025, 4, Downloaded from https://movementdisorders.onlinelibrary.wiley.com/doi/10.1002/mds.30104 by Mayo Clinic Libraries, Wiley Online Library on [07/09/2025]. See the Terms and Conditions (https://onlinelibrary.wiley.com/terms-and-conditions) on Wiley Online Library for rules of use; OA articles are governed by the applicable Creative Commons License

and slides were reviewed, confirming the presence of pTDP43 inclusions in both tissues. Slides were scanned using a ScanScope AT2 scanner (Leica Biosystems, Nussloch, Germany) at 40× magnification.

Protein Extraction from Postmortem Human Brain Tissues

A total of ~50 to 60 mg of caudate nucleus or substantia nigra were used to obtain RIPA-soluble and RIPA-insoluble fractions as previously described.[30] Samples were homogenized in 5× weight/volume of cold RIPA buffer (25 mM Tris–HCl, pH 7.6, 150 mM NaCl, 1% sodium deoxycholate, 1% Nonidet-P-40, 0.1% sodium dodecyl sulfate, and protease and phosphatase inhibitors at 1:100), sonicated on ice, and centrifuged at 100,000*g* for 30 minutes at 4°C. The supernatant generates the RIPA-soluble fraction. The protein concentration of the RIPA-soluble fraction was determined using bicinchoninic acid assay (Thermo Fisher). The remaining pellet was resuspended in RIPA buffer, sonicated, and centrifuged again to wash off any residual soluble proteins. The supernatant was discarded, and the remaining pellet was dissolved in urea buffer (30 mM Tris–HCl, pH 8.5, 7 M urea, 2 M thiourea, and 4% [(3-[(3-cholamidopropyl)-dimethylammonio]-1-propanesulfonate)]) for 1 hour at room temperature with continuous agitation. After incubation, the samples were sonicated and centrifuged at 100,000*g* for 30 minutes at 22°C. The resulting supernatant, referred as urea-soluble or RIPA-insoluble fraction, was then collected. The protein concentration of the urea-soluble fraction was determined by Bradford assay using the Pierce Coomassie Protein Assay Kit (Thermo Fisher).

pTDP-43 and HDGFL2 Cryptic Protein Immunoassay

pTDP-43 was assessed using the urea-soluble fraction from the caudate nucleus and substantia nigra of our study cohort using a sandwich Meso Scale Discovery (MSD) immunoassay. A novel rabbit monoclonal antibody specific for TDP-43 phosphorylated at serines 409/410 (3 µg/mL, in house monoclonal antibody 26H10[31]) was used for capture, and a novel goat polyclonal C-terminal TDP-43 antibody (3 µg/mL) paired with donkey anti-goat MSD SULFO-TAG antibody (1 µg/mL, R32AG-1, MSD) was used for detection. Levels of HDGFL2 cryptic protein in the caudate nucleus and substantia nigra were measured using the RIPA-soluble fraction, using a previously described MSD immunoassay.[29] Specifically, a commercial HDGFL2 antibody was biotinylated and used as the capture antibody (ProteinTech, 15134-1-AP, 4 µg/mL), and a novel antibody targeting the epitope generated by cryptic splicing of HDGFL2 was sulfo-tagged and used as the detection antibody (Mayo-LP, 4 µg/mL). MSD GOLD 96 Small Spot (L45_SA-1, MSD) streptavidin-coated plates were used in this assay. All samples were tested in duplicate wells, and controls were included in every plate to account for any interplate variability. MSD QUICKPLEX SQ120 technology was used to acquire the response values corresponding to the intensity of emitted light upon electrochemical stimulation.

Total RNA Extraction and Quantification from Postmortem Human Brain Tissues

RNA was extracted from human postmortem tissues of two different regions: caudate nucleus and substantia nigra. A total of ~40 mg of tissues was processed, using the RNeasy Plus Mini Kit (Qiagen), as previously described.[30] Briefly, tissues were manually homogenized (on ice) with pestles (Thermo Fisher) and 3-mL syringes with 21G × 1½ in. needles (BD Biosciences), in 600 µL of buffer RLT Plus supplemented with β-mercaptoethanol (1:100). Samples were centrifuged at 21,000*g* for 3 minutes at room temperature. The supernatant was then passed through gDNA eliminator columns, mixed with 70% ethanol, and placed in RNeasy MinElute Spin Columns to extract the RNA after centrifuging at 21,000*g* for 30 seconds at room temperature and applying different buffers provided by the kit. A DNAse I (Qiagen) in-column step was added to the protocol to ensure gDNA elimination. RNA was eluted using 20 µL of nuclease-free water, and its total concentration was determined using NanoDrop technology (NanoDrop One/OneC Microvolume UV–Vis. spectrophotometer; Thermo Fisher). RNA quality was assessed by measuring the RNA integrity number using an Agilent 2100 bioanalyzer (Agilent Technologies) (Table S1). Of note, we were unable to obtain high-quality RNA from substantia nigra of 4 controls, and from either caudate nucleus or substantia nigra from 1 of the 7 PS cases, and these were excluded from the analyses of cryptic RNAs and protein.

Complementary DNA Synthesis and Quantitative PCR

Complementary DNA (cDNA) synthesis was performed, using 500 ng of total RNA and the High-Capacity cDNA Transcription Kit with random primers (Applied Biosystems). The transcribed cDNA, diluted at 1:20 in RNAse/DNAse-free water, was used in quantitative polymerase chain reactions (qPCR) using SYBR GreenER qPCR SuperMix (Invitrogen, Thermo Fisher Scientific) on a QuantStudio 7 Flex RT-qPCR system. Control samples were included in every plate to account for any interplate variability. The samples were quantified using the ΔΔCt method and normalized to the housekeeping genes ribosomal protein lateral stalk subunit P0 (*RPLP0*) and glyceraldehyde-3-phosphate

15318257, 2025, 4, Downloaded from https://movementdisorders.onlinelibrary.wiley.com/doi/10.1002/mds.30104 by Mayo Clinic Libraries, Wiley Online Library on [07/09/2025]. See the Terms and Conditions (https://onlinelibrary.wiley.com/terms-and-conditions) on Wiley Online Library for rules of use; OA articles are governed by the applicable Creative Commons License

dehydrogenase (*GAPDH*). All primers used for this study are described in Table S2.

Statistical Analyses

Statistical analyses were performed in GraphPad Prism 9 (GraphPad Software). To evaluate the differences in pTDP-43 protein, HDGFL2 cryptic protein, cryptic RNA levels between PS, FTLD, and controls in the caudate nucleus and substantia nigra, or to determine the differences in cell marker levels between the caudate nucleus and substantia nigra, we performed a Kruskal–Wallis test followed by Dunn's multiple comparison test, as indicated in the figure legends. To adjust for age and sex differences in our study cohort, pTDP-43 differences were also assessed by multilinear regression analyses in which the reference group was either the control group (Table S3) or the PS cases to observe differences with the FTLD group (Table S4). To assess the differences in canonical RNA levels between the caudate nucleus and substantia nigra in controls, a Mann-Whitey *t* test was used. Spearman's associations were performed to determine the associations between pTDP-43, cellular markers, and/or cryptic RNA/protein levels.

Results

Evaluation and Quantification of TDP-43 Pathology

To evaluate the degree of TDP-43 dysfunction in PS brains, we obtained substantia nigra and caudate nucleus tissues from 7 PS cases, 12 FTLD cases with confirmed TDP-43 pathology, and 11 cognitively healthy controls (Table 1). We first validated the presence and distribution of TDP-43 inclusions in the brains of PS cases by performing immunohistochemistry for phosphorylated TDP-43 (pTDP-43). We found characteristic pTDP-43-positive inclusions in PS brains, including intranuclear inclusions (Fig. 1A), dendritic neurites (Fig. 1B), NCIs (Fig. 1C), glial cytoplasmic inclusions (Fig. 1D), and axonal spheroids (Fig. 1E). To quantify the burden of pTDP-43 pathology in both caudate nucleus and substantia nigra, we used an MSD-based immunoassay as previously described.[29-31] Compared to control brains, which lacked any detectable pTDP-43 in the detergent-insoluble protein lysates, the levels of pTDP-43 were significantly elevated in both the caudate nucleus and substantia nigra of PS brains (Fig. 1F). pTDP-43 levels in these regions remained significantly elevated compared to controls even after having adjusted for age and sex (Table S3). Similarly, pTDP-43 protein levels were significantly higher in the substantia nigra and caudate nucleus of FTLD cases compared to both controls and PS cases in unadjusted analysis and when controlling for age and sex differences (Fig. 1F; Table S4). However, no differences in pTDP-43 levels were observed for either PS or FTLD when brain regions were compared (Fig. 1F). Overall, we find a significant accumulation of pTDP-43 pathology in the substantia nigra and caudate nucleus of PS cases, to a lower extent than FTLD, and with a similar pTDP-43 burden between the two brain regions.

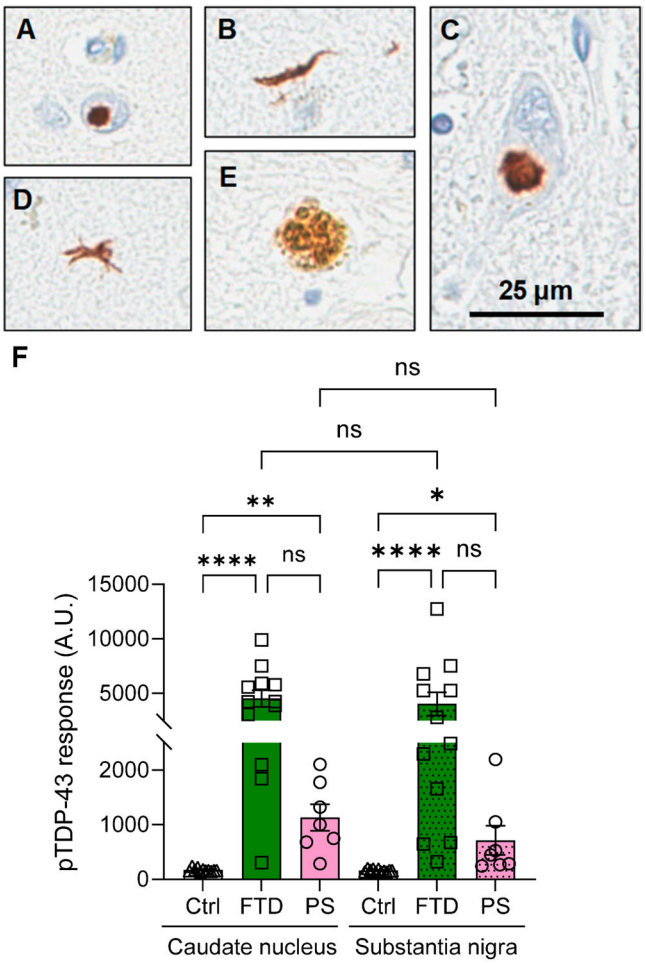

FIG. 1. TDP-43 (transactive-response DNA-binding protein of 43 kDa) pathology accumulates to a similar extent in the caudate nucleus and substantia nigra of PS (Perry syndrome) cases. Immunohistochemical staining of phosphorylated TDP-43 pathology in PS brains illustrating (**A**) intranuclear inclusions, (**B**) dendritic neurites, (**C**) neuronal cytoplasmic inclusions, (**D**) glial cytoplasmic inclusions, and (**E**) axonal spheroids. (**F**) Levels of pTDP-43 were measured by immunoassay in the detergent-insoluble, urea-soluble fraction extracted from the caudate nucleus and substantia nigra of PS, FTLD, and control (Ctrl) brains. Graph represents mean ± SEM (standard error of the mean). Statistical differences were assessed using nonparametric Kruskal–Wallis test followed by Dunn's multiple comparison test; $^{*}P < 0.05$, $^{**}P < 0.005$, $^{***}P < 0.001$, and $^{****}P < 0.0001$; ns, not significant. [Correction added on 21 February 2025, after first online publication: The figure 1 has been updated.] [Color figure can be viewed at wileyonlinelibrary.com]

Detection of TDP-43-Regulated Cryptic RNAs

Next, to determine the degree of TDP-43 splicing dysfunction in the caudate nucleus and substantia nigra

15318257, 2025, 4, Downloaded from https://movementdisorders.onlinelibrary.wiley.com/doi/10.1002/mds.30104 by Mayo Clinic Libraries, Wiley Online Library on [07/09/2025]. See the Terms and Conditions (https://onlinelibrary.wiley.com/terms-and-conditions) on Wiley Online Library for rules of use; OA articles are governed by the applicable Creative Commons License

of PS brains, we evaluated the levels of the following eight cryptic (or skiptic in the case of *KCNQ2*) RNAs using quantitative reverse transcription PCR (qRT-PCR): actin-like 6B (*ACTL6B*), calcium/calmodulin-dependent protein kinase II β (*CAMK2B*), stathmin 2 (*STMN2*), unc-13 homolog A (*UNC13A*), potassium voltage-gated channel subfamily Q member 2 (*KCNQ2*), autophagy-related 4B cysteine peptidase (*ATG4B*), G protein signaling modulator 2 (*GPSM2*), and hepatoma-derived growth factor–related protein 2 (*HDGFL2*). These cryptic RNAs were selected based on prior validation in FTLD and AD brains.[22,26,28,30] Further, they represent both neuronal (*ACTL6B*, *CAMK2B*, *STMN2*, *UNC13A*, and *KCNQ2*) and nonneuronal (*ATG4B*, *GPSM2*, and *HDGFL2*) targets (Fig. S1[32]) that are sensitive to TDP-43 dysfunction.[18,20,28] Additionally, some targets have high relevance to disease mechanisms (*STMN2* and *UNC13A*),[33-38] and others are potential biomarker candidates as they produce proteins with novel epitopes that have been detected in the cerebrospinal fluid (CSF) of ALS/FTLD cases (CAMK2B, KCNQ2, and HDGFL2).[28,39]

In FTLD, the levels of all TDP-43-regulated cryptic RNAs evaluated were significantly increased in the caudate nucleus compared to controls, and *STMN2*, *UNC13A*, *KCNQ2*, *ATG4B*, and *GPSM2* were significantly upregulated in the substantia nigra (Fig. 2A,B). In PS caudate nucleus, all cryptic targets tested were also significantly increased compared to control levels (Fig. 2A,B). Interestingly, in the caudate nucleus, the levels of cryptic RNAs were not significantly different between PS and FTLD (Fig. 2A,B). Unexpectedly, only *UNC13A* cryptic RNA was significantly elevated in the substantia nigra of PS (Fig. 2A). Other targets were unchanged in the PS substantia nigra compared to controls, although we observed trends toward increased levels of *GPSM2* cryptic RNA, which is more broadly expressed (Fig. 2B). Overall, we find that cryptic RNAs characteristic of FTLD are also elevated in the caudate nucleus of PS. Further, we find differences in the cryptic RNAs identified between regions in both PS and FTLD despite similar levels of pTDP-43 pathology.

Detection of TDP-43-Regulated HDGFL2 Cryptic Protein

Recent studies have highlighted the potential of de novo proteins obtained from TDP-43-mediated cryptic splicing as surrogate markers of TDP-43 dysfunction. Cryptic splicing of *HDGFL2* RNA leads to an in-frame insertion of an intronic sequence and the production of a stable transcript and cryptic protein (Fig. 2C), which is detected in the affected brain regions and the CSF of ALS/frontotemporal dementia (FTD) patients,[28,29,39] demonstrating its potential utility as a biomarker and readout of TDP-43 function. Using a previously established immunoassay that uses an antibody targeting the novel epitope of the HDGFL2 cryptic protein,[29] we found elevated levels in the caudate nucleus of both PS and FTLD compared to control brains (Fig. 2C). In the substantia nigra, HDGFL2 cryptic protein was not elevated in either group compared to controls (Fig. 2C).

Assessing Associations between Cryptic RNA or Protein Levels and TDP-43 Pathology

Previous studies have shown that the accumulation of TDP-43-regulated cryptic RNAs associates with pTDP-43 protein levels.[29,30] Thus, we next evaluated whether cryptic RNA or protein burden associated with pTDP-43 deposition in the caudate nucleus and substantia nigra (Figs. S2 and S3). In the caudate nucleus, only cryptic *ATG4B* and skiptic *KCNQ2* levels significantly associated with pTDP-43 protein burden in PS and FTLD, respectively (Fig. S2A,B). The levels of HDGFL2 cryptic protein significantly associated with pTDP-43 levels in PS caudate but not in FTLD (Fig. S2C). We had observed the accumulation of only some cryptic RNAs in the substantia nigra for FTLD and only one in PS (Fig. 2), and consistently found limited associations with cryptic RNAs and pTDP-43 in this region (Fig. S3). Indeed, the only significant association was between *GPSM2* cryptic RNA and pTDP-43 protein levels in FTLD cases (Fig. 3B). Overall, we find limited correlations between the levels of cryptic RNAs and pTDP-43 pathology in either region of PS or FTLD brains.

Cell-Type Compositions between Regions May Explain Differences in Cryptic RNA Accumulation

To attempt to understand the underlying differences in cryptic splicing in the caudate nucleus and substantia nigra, we investigated the cell-type composition of these regions. We performed qRT-PCR to measure the levels of neuronal (*RBFOX3*),[40,41] microglial (*TMEM119*),[42] astrocytic (*GFAP*),[43] and oligodendrocytic (*OLIG2*)[44] specific genes (Fig. 3A[32]). The levels of the neuronal marker *RBFOX3* were significantly lower in the substantia nigra compared to the caudate nucleus for PS, FTLD, and controls (Fig. 3B). Conversely, the astrocyte marker, *GFAP*, was higher in the substantia nigra compared to the caudate nucleus, with significant increases observed in PS and control brains (Fig. 3C). Oligodendrocyte marker *OLIG2* was significantly increased in FTLD brains (Fig. 3D), and microglial transcript levels were comparable between both regions for all groups (Fig. 3E). Additionally, the levels of certain canonical neuronal RNAs (*CAMK2B*, *UNC13A*, and *KCNQ2*) were decreased in the substantia nigra compared to the caudate nucleus (Fig. S4). These results are consistent

15318257, 2025, 4, Downloaded from https://movementdisorders.onlinelibrary.wiley.com/doi/10.1002/mds.30104 by Mayo Clinic Libraries, Wiley Online Library on [07/09/2025]. See the Terms and Conditions (https://onlinelibrary.wiley.com/terms-and-conditions) on Wiley Online Library for rules of use; OA articles are governed by the applicable Creative Commons License

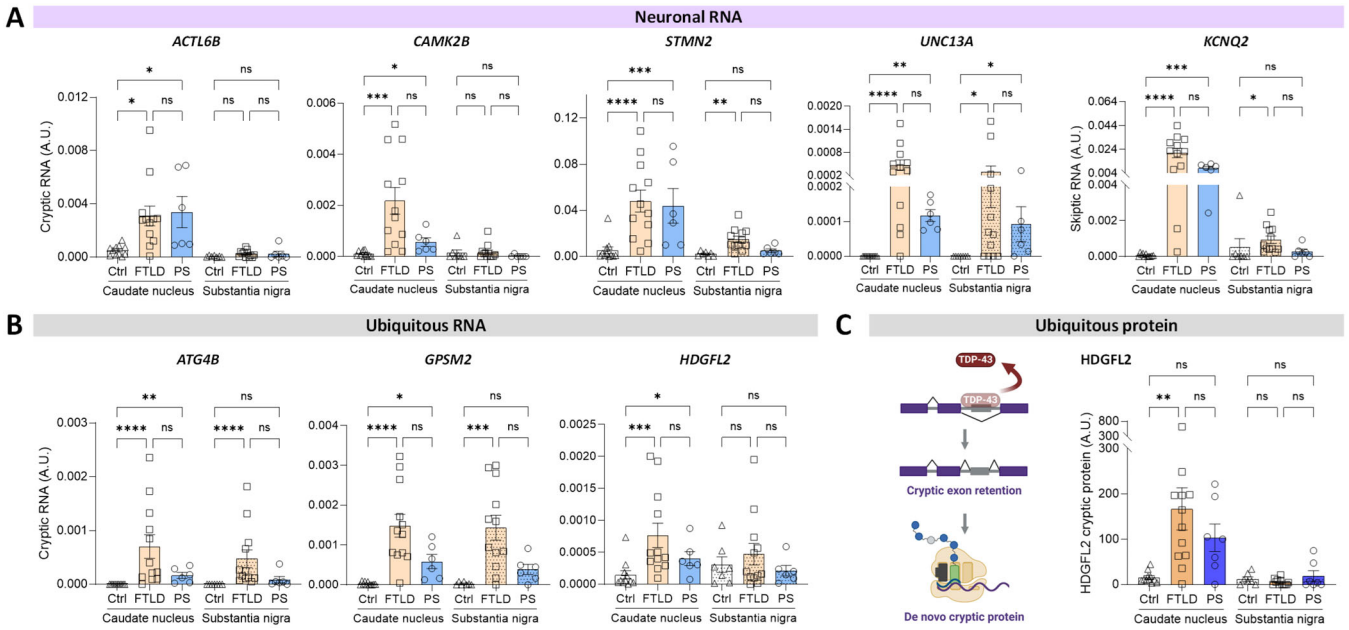

FIG. 2. Certain TDP-43 (transactive-response DNA-binding protein of 43 kDa) cryptic (or skiptic) RNAs targets are upregulated in PS (Perry syndrome) caudate nucleus. The levels of (**A**) neuronal cryptic RNAs and skiptic neuronal RNA, (**B**) more ubiquitous RNAs, or (**C**) HDGFL2 cryptic protein were measured from the caudate nucleus and substantia nigra of PS, FTLD, and control (Ctrl) cases. Graphs represent mean ± SEM (standard error of the mean). Statistical differences were assessed using nonparametric Kruskal–Wallis test followed by Dunn's multiple comparison test; $^{*}P < 0.05$, $^{**}P < 0.005$, $^{***}P < 0.001$, and $^{****}P < 0.0001$; ns, not significant. [Color figure can be viewed at wileyonlinelibrary.com]

with lower *RBFOX3* RNA in the substantia nigra compared to the caudate nucleus. Conversely, more ubiquitously expressed targets (*ATG4B* and *GPSM2*), or the highly abundant *STMN2* RNA, were similarly expressed in both regions (Fig. S4). Despite the lack of differences in overall transcript expression between brain regions, cryptic variants for *STMN2*, *ATG4B*, or *GPSM2* did not accumulate in PS substantia nigra. Thus, although some transcripts are more highly expressed in the caudate nucleus, transcript abundance alone does not fully explain the differences in cryptic splicing detected between regions. Overall, we find key differences in the cellular compositions and canonical RNA expression of the caudate nucleus compared to the substantia nigra, which may contribute to the regional disparities in cryptic RNAs identified.

Next, we hypothesized that pTDP-43 accumulation and cryptic RNAs or HDGFL2 cryptic protein may associate with changes in RNA levels of specific cell types susceptible to TDP-43 pathology. In FTLD caudate nucleus or substantia nigra, pTDP-43 protein levels did not significantly associate strongly with any cell-type marker, except that we observed a trend toward a positive correlation with the microglial marker, *TMEM119*, in the substantia nigra (Fig. S5). Similarly, we did not find significant correlations between pTDP-43 and cell marker RNAs in PS, but pTDP-43 protein and *GFAP* RNA levels trended toward positive correlation in both the caudate nucleus and substantia nigra (Fig. S6). HDGFL2 cryptic protein levels correlated with *GFAP* RNA levels in the caudate nucleus of FTLD cases (Fig. S7). Our findings that the array of cryptic RNAs differ between brain regions and diseases may provide important insights into TDP-43-dependent disease mechanisms.

Discussion

In this study, we sought to evaluate the extent to which TDP-43 dysfunction is present in the rare neurodegenerative disease of PS. Quantification of the levels of detergent-insoluble pTDP-43 protein revealed a significant and similar accumulation between the caudate nucleus and substantia nigra in both PS and FTLD. The clinical significance of TDP-43 inclusions in the substantia nigra of FTLD cases has not been fully resolved but may be involved in clinical heterogeneity and has been associated with increased frequency of movement disorders in FTLD.[14]

TDP-43 mislocalization and depletion from the nucleus as seen in FTLD/ALS and AD lead to the accumulation of cryptic RNAs, which significantly correlate with insoluble pTDP-43 protein levels in affected regions (frontal cortex, amygdala, and hippocampus).[22,26,29,30] In PS and FTLD, we observed differences in the cryptic RNA signature between diseases (in the substantia nigra) as well as between anatomical regions within each disease. In the caudate nucleus of FTLD and PS cases all eight (*ACTL6B*, *CAMK2B*, *STMN2*,

15318257, 2025, 4, Downloaded from https://movementdisorders.onlinelibrary.wiley.com/doi/10.1002/mds.30104 by Mayo Clinic Libraries, Wiley Online Library on [07/09/2025]. See the Terms and Conditions (https://onlinelibrary.wiley.com/terms-and-conditions) on Wiley Online Library for rules of use; OA articles are governed by the applicable Creative Commons License

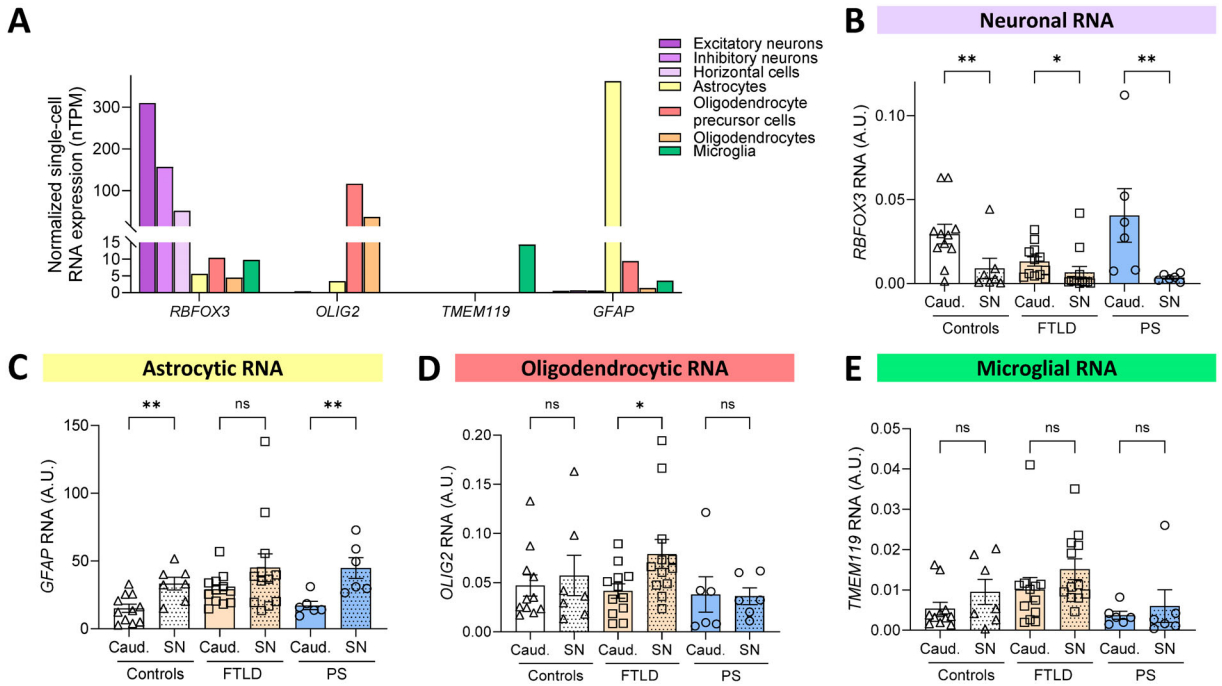

FIG. 3. Cell-type composition may explain differential accumulation of cryptic RNAs within certain brain regions but does not explain differences across brain regions. (**A**) RNA expression values were derived from The Human Protein Atlas[32] for the cell types and transcripts shown. RNA levels of (**B**) neuronal (*RBFOX3*), (**C**) astrocytic (*GFAP*), (**D**) oligodendrocytic (*OLG2*), and (**E**) microglial (*TMEM119*) markers were measured using qRT-PCR. Caud., caudate nucleus; SN, substantia nigra. Graphs represent mean ± SEM (standard error of the mean). Statistical differences were assessed using nonparametric Kruskal–Wallis test followed by Dunn's multiple comparison test; *$P < 0.05$, **$P < 0.005$, ***$P < 0.001$, and ****$P < 0.0001$; ns, not significant. [Color figure can be viewed at wileyonlinelibrary.com]

UNC13A, *KCNQ2*, *ATG4B*, *GPSM2*, and *HDGFL2*) TDP-43 cryptic RNA and HDGFL2 cryptic protein targets were upregulated. Five cryptic RNAs (*STMN2*, *UNC13A*, *KCNQ2*, *ATG4B*, and *GPSM2*) were identified in the substantia nigra of FTLD patients, whereas only *UNC13A* was detected in PS.

In both FTLD and PS, a higher number of cryptic targets were significantly upregulated, compared to controls, in the caudate nucleus versus the substantia nigra. This regional variation cannot be explained by pathological burden and/or target sensitivity, as the overall levels of pTDP-43 protein were similar between regions in FTLD and PS. Additionally, the levels of certain ubiquitously expressed canonical transcripts remain unchanged between regions in controls. Interestingly, interrogation of cell-type composition in both tissues revealed a stark difference, with increased neuronal *RBFOX3* (also known as NeuN) RNA levels in the caudate nucleus and increased expression of astrocytic or oligodendrocytic transcripts in the substantia nigra of PS and FTLD, respectively. In line with our findings, neuronal immunoreactivity (NeuN) in the substantia nigra has been reported to be heterogenous and lower than other brain regions.[45] All neuronal targets measured in this study were previously identified from NeuN-positive/TDP-43-negative nuclei isolated from FTLD/ALS patients or neuronal cultures in which TDP-43 had been downregulated.[23,26,28] Thus, NeuN-associated cryptic RNAs may not fully represent the extent of TDP-43 dysfunction in different affected regions and/or diseases. In fact, differences in cell composition as well as transcriptome differences have been reported between frontal and temporal cortex as well as the cerebellum in FTLD with TDP-43 proteinopathy.[46] Further, previous mouse studies have unequivocally demonstrated a cell-type-specific landscape of cryptic targets in neurons versus skeletal muscle, stems cells, oligodendrocytic lineage cells, and Schwann cells,[21,47,48] supporting the existence of region-specific effects in disease.

Interestingly, TDP-43 pathology in PS, compared to FTLD, is more glial in nature.[1,12,13] Despite few overall correlations with pTDP-43 burden and cryptic RNAs observed, we found associations between pTDP-43 protein levels and some cryptic targets with astrocyte marker levels (*GFAP*) in PS. It is tempting to speculate that TDP-43 dysfunction may be represented by glial-specific or more ubiquitously expressed cryptic targets. However, because TDP-43-regulated cryptic RNAs are not evolutionarily conserved, studies exploring nonneuronal and neuronal subtype-specific cryptic targets in humans are warranted and will be increasingly feasible with emerging technologies, including single-cell sequencing combined with long-read sequencing as well spatial transcriptomics.

Apart from target abundance, pathological burden, sensitivity of targets to TDP-43 loss, and differences in

15318257, 2025, 4, Downloaded from https://movementdisorders.onlinelibrary.wiley.com/doi/10.1002/mds.30104 by Mayo Clinic Libraries, Wiley Online Library on [07/09/2025]. See the Terms and Conditions (https://onlinelibrary.wiley.com/terms-and-conditions) on Wiley Online Library for rules of use; OA articles are governed by the applicable Creative Commons License

cell-type composition of tissues, we speculate that the expression of splicing modulators may regulate cryptic splicing and contribute to cell-type/regional heterogeneity. Previous work supports this notion, finding that other RNA binding proteins (RBP) repress cryptic exon splicing of *UNC13A* independently of TDP-43.[49] Similarly, cell-type-specific expression of RBPs differentially modulate cryptic exon inclusion in cultured mouse neuroblastoma versus skeletal muscle cells.[50] Thus, a more complete understanding of how cryptic splicing is regulated within neuronal and nonneuronal cells across different regions is necessary and may provide insight into mechanisms of selective vulnerability of certain regions to TDP-43 dysfunction in TDP-43 proteinopathies.

Cryptic splicing of *HDGFL2* transcript results in the production of a stable cryptic protein that can be detected in the affected brain regions and CSF using mass spectrometry and antibodies recognizing the novel cryptic epitope.[28,29,39] Using one of these recently produced antibodies we found that HDGFL2 cryptic protein levels were significantly elevated compared to controls in the caudate nucleus of FTLD and PS cases. Further, HDGFL2 cryptic protein level correlated with pTDP-43 burden in PS caudate nucleus. Conversely, HDGFL2 cryptic protein was not detected in the substantia nigra. Nonetheless, HDGFL2 cryptic protein upregulation in the caudate nucleus and potential release from affected cells into the CSF and blood suggest that it may serve as a biomarker of TDP-43 activity in PS. Of interest, cryptic RNA accumulation resulting from TDP-43 dysfunction can be detected even in the absence of TDP-43 inclusions.[20,51] Similarly, HDGFL2 cryptic protein, even more so than its RNA, is highly correlated with pTDP-43 protein levels and can discriminate between AD cases with and without TDP-43 pathology,[29] suggesting that cryptic RNAs and HDGFL2 cryptic protein are highly sensitive to TDP-43 loss of function, which likely precedes overt aggregation.

Our detection of cryptic splicing of many transcripts nominates novel disease mechanisms and potential therapeutic targets in PS. Unexpectedly, only one cryptic target, *UNC13A*, was detected in the PS substantia nigra, the brain region in PS with high amounts of pathology and neurodegeneration. UNC13A loss of function likely plays a significant role in the pathogenesis of ALS/FTD, as a single-nucleotide polymorphism located within the cryptic exon shortens disease duration, by exacerbating cryptic splicing and altering synaptic activity.[25,26,36-38] Whether UNC13A loss of function contributes to neurodegeneration in the substantia nigra of PS will require further study. We also highlight that the neuronal composition of the substantia nigra is very different from the caudate nucleus hinting of the possibility of novel RNA clients of TDP-43 in this region that have yet to be identified. Additionally, to what degree targets in the caudate nucleus are involved in PS requires further exploration. Recently, splice modulating antisense oligonucleotides (ASO) to restore splicing and expression of TDP-43 targets, including *UNC13A*, have proved successful in cell and animal models, and are being actively pursued for the treatment of ALS and potentially FTLD.[36,38,52] Moreover, a novel modality of precision medicine, leveraging TDP-43 cryptic splicing, has been described. TDP-REG constructs use cryptic splicing induced by a loss of TDP-43 activity to express a protein with a therapeutic potential only in affected cells.[38] The link between PS and TDP-43 misprocessing of key targets may hold promise to a better understanding of disease mechanisms and with the description of ASOs and tools for precision medicine in the context of TDP-43 dysregulation may offer multiple tools for the treatment of PS.

Despite identifying TDP-43-mediated splicing dysfunction in PS and regional variation in cryptic splicing in both FTLD and PS, this study has some limitations. Due to PS being an extremely rare disease and the challenges of obtaining post-mortem tissues for research, the total number of individuals with PS included in this study was quite significant, although it may be underpowered to detect significant elevation of some cryptic RNAs or correlations between them and TDP-43 pathology. Indeed, we detected few significant associations of cryptic RNA targets and pTDP-43 levels that could be due to sample size or differences in the expression of target transcripts between regions and within cell types, which will be an important future direction to fully understand regional specificity of cryptic splicing. Nonetheless, our findings will be of interest to the research community. Our analyses focused on two regions affected in PS and exhibiting significant TDP-43 pathology, the substantia nigra and caudate nucleus. However, other brain regions implicated in PS may also harbor cryptic RNAs due to TDP-43 dysfunction, even in the absence of abundant TDP-43 inclusions, supporting continued research efforts in this area.

In conclusion, we identified cryptic RNA and protein that accumulate in the caudate nucleus of PS cases resulting from TDP-43 dysfunction. Further, we provide evidence of differential cryptic regulation between diseases and, interestingly, between brain regions. Given the importance of cryptic exon biology in the development of biomarkers to identify patients with TDP-43 pathology,[28,29,39] as well as targets for therapeutic intervention in different TDP-43 proteinopathies, it is imperative we identify which cryptic splicing events are common and which may be disease specific. Further, an in-depth understanding of the consequences of TDP-43 dysfunction across different brain regions may shed light on selective vulnerability in these diverse diseases.

15318257, 2025, 4, Downloaded from https://movementdisorders.onlinelibrary.wiley.com/doi/10.1002/mds.30104 by Mayo Clinic Libraries, Wiley Online Library on [07/09/2025]. See the Terms and Conditions (https://onlinelibrary.wiley.com/terms-and-conditions) on Wiley Online Library for rules of use; OA articles are governed by the applicable Creative Commons License

Author Roles: (1) Research project: A. Conception, B. Organization, C. Execution; (2) Statistical analysis: A. Design, B. Execution, C. Review and critique; (3) Manuscript: A. Writing of the first draft, B. Review and critique.
S.R.P.: 1B, 2A, 2C, 3A, 3B
J.G.B.: 1C, 2B, 3A, 3B
A.N.: 1C, 3A
L.D.: 1C
C.M.C.: 1C, 2B, 3B
M.M.R.: 2A, 2C, 3B
M.Y.: 1C
P.C.O.: 1C
V.E.A.: 1C
J.D.: 1B, 3B
Y.S.: 1B, 1C
J.T.: 1B, 1C
M.D.: 1B
B.R.: 1B
M.C.-C.: 1B, 1C
J.D.: 1B, 3B
C.C.-C.: 1B, 3B
Y.Z.: 1B, 3B
K.A.J.: 1B, 3B
D.W.D.: 1A, 1B, 3B
L.P.: 1A, 1B, 3B
Z.K.W.: 1B, 3B
M.P.: 1A, 1B, 1C, 2A, 2B, 2C, 3A, 3B

Acknowledgments: We extend our heartfelt gratitude to the patients and their families for their invaluable contributions to this study. We are also grateful to Ms. Audrey Strongosky for her assistance with the logistics of brain specimen procurement. Additionally, we thank Wanhao Chi and Evangelos Kiskinis for their expertise in designing and sharing the *KCNQ2* qRT-PCR primers. The graphical abstract and the diagram in Figure 2C were created using BioRender.com.

Full financial disclosures of all authors for the preceding 12 months: J.D. serves as an editorial board member of Neurologia i Neurochirurgia Polska. J.D. received a speakers' bureau honoraria from VM Media Ltd., Radosław Lipiński 90 Consulting, and Ipsen. J.D. has intellectual property rights for "Application of Hydrogen Peroxide and 17β-Estradiol and Its Metabolites as Biomarkers in a Method of Diagnosing Neurodegenerative Diseases In Vitro" (WO/2023/234790).
Z.K.W. serves as a principal investigator (PI) or co-PI for Biohaven Pharmaceuticals, Inc. (BHV4157-206); Vigil Neuroscience, Inc. (VGL101-01.002, VGL101-01.201, PET tracer development protocol, CSFR1R biomarker and repository project, and ultra-high field MRI in the diagnosis and management of CSF1R-related adult-onset leukoencephalopathy with axonal spheroids and pigmented glia); ONO-2808-03; and Amylyx AMX0035-009 projects/grants. He serves as co-PI of the Mayo Clinic APDA Center for Advanced Research and as an external advisory board member for Vigil Neuroscience, Inc., and as a consultant for Eli Lilly & Company and for NovoGlia, Inc.
L.P. is a consultant for Expansion Therapeutics.

Data Availability Statement

The data generated or analyzed in the current study are included in this published article and its supplementary information files available, or available from the corresponding author upon reasonable request.

References

1. Wider C, Dickson DW, Stoessl AJ, et al. Pallidonigral TDP-43 pathology in Perry syndrome. Parkinsonism Relat Disord 2009;15:281–286.
2. Wider C, Wszolek ZK. Rapidly progressive familial parkinsonism with central hypoventilation, depression and weight loss (Perry syndrome)—a literature review. Parkinsonism Relat Disord 2008;14:1–7.
3. Mishima T, Fujioka S, Tomiyama H, et al. Establishing diagnostic criteria for Perry syndrome. J Neurol Neurosurg Psychiatry 2018;89:482–487.
4. Wider C, Dachsel JC, Farrer MJ, Dickson DW, Tsuboi Y, Wszolek ZK. Elucidating the genetics and pathology of Perry syndrome. J Neurol Sci 2010;289:149–154.
5. Dulski J, Konno T, Wszolek Z. DCTN1-related neurodegeneration. In: Adam MP, Feldman J, Mirzaa GM, et al., eds. GeneReviews ((R)). Seattle (WA): University of Washington; 1993-2024.
6. Dulski J, Ross OA, Wszolek ZK. Genetics of Parkinson's disease: state-of-the-art and role in clinical settings. Neurol Neurochir Pol 2024;58:38–46.
7. Dulski J, Cerquera-Cleves C, Milanowski L, et al. Clinical, pathological and genetic characteristics of Perry disease-new cases and literature review. Eur J Neurol 2021;28:4010–4021.
8. Perry TL, Bratty PJA, Hansen S, Kennedy J, Urquhart N, Dolman CL. Hereditary mental depression and parkinsonism with taurine deficiency. Arch Neurol 1975;32:108–113.
9. Farrer MJ, Hulihan MM, Kachergus JM, et al. DCTN1 mutations in Perry syndrome. Nat Genet 2009;41:163–165.
10. Gustavsson EK, Trinh J, Guella I, et al. DCTN1 p.K56R in progressive supranuclear palsy. Parkinsonism Relat Disord 2016;28:56–61.
11. Felicio AC, Dinelle K, Agarwal PA, et al. In vivo dopaminergic and serotonergic dysfunction in DCTN1 gene mutation carriers. Mov Disord 2014;29:1197–1201.
12. Mishima T, Koga S, Lin WL, et al. Perry syndrome: a distinctive type of TDP-43 Proteinopathy. J Neuropathol Exp Neurol 2017;76:676–682.
13. Lin WL, Castanedes-Casey M, Dickson DW. Transactivation response DNA-binding protein 43 microvasculopathy in frontotemporal degeneration and familial Lewy body disease. J Neuropathol Exp Neurol 2009;68:1167–1176.
14. Fiondella L, Gami-Patel P, Blok CA, et al. Movement disorders are linked to TDP-43 burden in the substantia nigra of FTLD-TDP brain donors. Acta Neuropathol Commun 2023;11:63.
15. Josephs KA, Stroh A, Dugger B, Dickson DW. Evaluation of subcortical pathology and clinical correlations in FTLD-U subtypes. Acta Neuropathol 2009;118:349–358.
16. Mackenzie IR, Neumann M. Subcortical TDP-43 pathology patterns validate cortical FTLD-TDP subtypes and demonstrate unique aspects of C9orf72 mutation cases. Acta Neuropathol 2020;139:83–98.
17. Lagier-Tourenne C, Polymenidou M, Cleveland DW. TDP-43 and FUS/TLS: emerging roles in RNA processing and neurodegeneration. Hum Mol Genet 2010;19:R46–R64.
18. Ling JP, Pletnikova O, Troncoso JC, Wong PC. TDP-43 repression of nonconserved cryptic exons is compromised in ALS-FTD. Science 2015;349:650–655.
19. Mehta PR, Brown AL, Ward ME, Fratta P. The era of cryptic exons: implications for ALS-FTD. Mol Neurodegener 2023;18:16.
20. Sun M, Bell W, LaClair KD, et al. Cryptic exon incorporation occurs in Alzheimer's brain lacking TDP-43 inclusion but exhibiting nuclear clearance of TDP-43. Acta Neuropathol 2017;133:923–931.
21. Jeong YH, Ling JP, Lin SZ, et al. Tdp-43 cryptic exons are highly variable between cell types. Mol Neurodegener 2017;12:13.
22. Prudencio M, Humphrey J, Pickles S, et al. Truncated stathmin-2 is a marker of TDP-43 pathology in frontotemporal dementia. J Clin Invest 2020;130:6080–6092.
23. Melamed Z, Lopez-Erauskin J, Baughn MW, et al. Premature polyadenylation-mediated loss of stathmin-2 is a hallmark of TDP-43-dependent neurodegeneration. Nat Neurosci 2019;22:180–190.
24. Klim JR, Williams LA, Limone F, et al. ALS-implicated protein TDP-43 sustains levels of STMN2, a mediator of motor neuron growth and repair. Nat Neurosci 2019;22:167–179.
25. Brown AL, Wilkins OG, Keuss MJ, et al. TDP-43 loss and ALS-risk SNPs drive mis-splicing and depletion of UNC13A. Nature 2022;603:131–137.
26. Ma XR, Prudencio M, Koike Y, et al. TDP-43 represses cryptic exon inclusion in the FTD-ALS gene UNC13A. Nature 2022;603:124–130.

15318257, 2025, 4, Downloaded from https://movementdisorders.onlinelibrary.wiley.com/doi/10.1002/mds.30104 by Mayo Clinic Libraries, Wiley Online Library on [07/09/2025]. See the Terms and Conditions (https://onlinelibrary.wiley.com/terms-and-conditions) on Wiley Online Library for rules of use; OA articles are governed by the applicable Creative Commons License

27. Torres P, Ramirez-Nunez O, Romero-Guevara R, et al. Cryptic exon splicing function of TARDBP interacts with autophagy in nervous tissue. Autophagy 2018;14:1398–1403.

28. Seddighi S, Qi YA, Brown AL, et al. Mis-spliced transcripts generate de novo proteins in TDP-43-related ALS/FTD. Sci Transl Med 2024; 16(734):eadg7162.

29. Calliari A, Daughrity LM, Albagli EA, et al. HDGFL2 cryptic proteins report presence of TDP-43 pathology in neurodegenerative diseases. Mol Neurodegener 2024;19:29.

30. Estades Ayuso V, Pickles S, Todd T, et al. TDP-43-regulated cryptic RNAs accumulate in Alzheimer's disease brains. Mol Neurodegener 2023;18:57.

31. Castellanos Otero P, Todd TW, Shao W, et al. Generation and characterization of monoclonal antibodies against pathologically phosphorylated TDP-43. PLoS One 2024;19:e0298080.

32. Karlsson M, Zhang C, Mear L, et al. A single-cell type transcriptomics map of human tissues. Sci Adv 2021;7(31):eabh2169.

33. Lopez-Erauskin J, Bravo-Hernandez M, Presa M, et al. Stathmin-2 loss leads to neurofilament-dependent axonal collapse driving motor and sensory denervation. Nat Neurosci 2024;27:34–47.

34. Krus KL, Strickland A, Yamada Y, et al. Loss of Stathmin-2, a hallmark of TDP-43-associated ALS, causes motor neuropathy. Cell Rep 2022;39:111001.

35. Guerra San Juan I, Nash LA, Smith KS, et al. Loss of mouse Stmn2 function causes motor neuropathy. Neuron 2022;110(1671–1688): e1676.

36. Keuss MJ, Harley P, Ryadnov E, et al. Loss of TDP-43 Induces Synaptic Dysfunction That is Rescued by UNC13A Splice-Switching ASOs. Long Island, NY: Cold Spring Harbor Laboratory; 2024.

37. Diekstra FP, van Vught PW, van Rheenen W, et al. UNC13A is a modifier of survival in amyotrophic lateral sclerosis. Neurobiol Aging 2012;33(630):e633–e638.

38. Wilkins OG, Chien M, Wlaschin JJ, et al. Creation of de novo cryptic splicing for ALS and FTD precision medicine. Science 2024;386: 61–69.

39. Irwin KE, Jasin P, Braunstein KE, et al. A fluid biomarker reveals loss of TDP-43 splicing repression in presymptomatic ALS-FTD. Nat Med 2024;30:382–393.

40. Mullen RJ, Buck CR, Smith AM. NeuN, a neuronal specific nuclear protein in vertebrates. Development 1992;116:201–211.

41. Kim KK, Adelstein RS, Kawamoto S. Identification of neuronal nuclei (NeuN) as Fox-3, a new member of the Fox-1 gene family of splicing factors. J Biol Chem 2009;284:31052–31061.

42. Bennett ML, Bennett FC, Liddelow SA, et al. New tools for studying microglia in the mouse and human CNS. Proc Natl Acad Sci U S A 2016;113:E1738–E1746.

43. Yang Z, Wang KK. Glial fibrillary acidic protein: from intermediate filament assembly and gliosis to neurobiomarker. Trends Neurosci 2015;38:364–374.

44. Ligon KL, Fancy SP, Franklin RJ, Rowitch DH. Olig gene function in CNS development and disease. Glia 2006;54:1–10.

45. Gusel'nikova VV, Korzhevskiy DE. NeuN As a neuronal nuclear antigen and neuron differentiation marker. Acta Naturae 2015;7: 42–47.

46. Hasan R, Humphrey J, Bettencourt C, et al. Transcriptomic analysis of frontotemporal lobar degeneration with TDP-43 pathology reveals cellular alterations across multiple brain regions. Acta Neuropathol 2022;143:383–401.

47. Heo D, Ling JP, Molina-Castro GC, et al. Stage-specific control of oligodendrocyte survival and morphogenesis by TDP-43. eLife 2022;11:e75230.

48. Chang KJ, Agrawal I, Vainshtein A, et al. TDP-43 maximizes nerve conduction velocity by repressing a cryptic exon for paranodal junction assembly in Schwann cells. eLife 2021;10:e64456.

49. Koike Y, Pickles S, Estades Ayuso V, et al. TDP-43 and other hnRNPs regulate cryptic exon inclusion of a key ALS/FTD risk gene, UNC13A. PLoS Biol 2023;21:e3002028.

50. Susnjar U, Skrabar N, Brown AL, et al. Cell environment shapes TDP-43 function with implications in neuronal and muscle disease. Commun Biol 2022;5:314.

51. Pickles S, Gendron TF, Koike Y, et al. Evidence of cerebellar TDP-43 loss of function in FTLD-TDP. Acta Neuropathol Commun 2022;10:107.

52. Baughn MW, Melamed Z, Lopez-Erauskin J, et al. Mechanism of STMN2 cryptic splice-polyadenylation and its correction for TDP-43 proteinopathies. Science 2023;379:1140–1149.

Supporting Data

Additional Supporting Information may be found in the online version of this article at the publisher's web-site.

15318257, 2025, 4, Downloaded from https://movementdisorders.onlinelibrary.wiley.com/doi/10.1002/mds.30104 by Mayo Clinic Libraries, Wiley Online Library on [07/09/2025]. See the Terms and Conditions (https://onlinelibrary.wiley.com/terms-and-conditions) on Wiley Online Library for rules of use; OA articles are governed by the applicable Creative Commons License